Trends in Analytical Chemistry 175 (2024) 117713

Contents lists available at ScienceDirect

Trends in Analytical Chemistry

journal homepage: www.elsevier.com/locate/trac

Frontiers in mass spectrometry-based spatial metabolomics: Current applications and challenges in the context of biomedical research

Kate Wheeler [a,1], Camil Gosmanov [b,1], Michael Jimenez Sandoval [c], Zhibo Yang [b], Laura-Isobel McCall [b,d,*]

[a] Department of Biology, University of Oklahoma, 101 Stephenson Parkway, Norman, OK, 73019, USA
[b] Department of Chemistry and Biochemistry, University of Oklahoma, 101 Stephenson Parkway, Norman, OK, 73019, USA
[c] Neuroscience Program, Amherst College, 5 East Drive, Amherst, MA, 01002, USA
[d] Department of Chemistry and Biochemistry, San Diego State University, 5500 Campanile Drive, San Diego, CA, 92182, USA

ARTICLE INFO

Keywords:
Mass spectrometry
Metabolomics
Spatial analysis
MALDI mass spectrometry imaging
DESI mass spectrometry imaging
Secondary ion mass spectrometry
Chemical cartography

ABSTRACT

Metabolites are critical products and mediators of cellular and tissue function, and key signals in cell-to-cell, organ-to-organ and cross-organism communication. Many of these interactions are spatially segregated. Thus, spatial metabolomics can provide valuable insight into healthy tissue function and disease pathogenesis. Here, we review major mass spectrometry-based spatial metabolomics techniques and the biological insights they have enabled, with a focus on brain and microbiota function and on cancer, neurological diseases and infectious diseases. These techniques also present significant translational utility, for example in cancer diagnosis, and for drug development. However, spatial mass spectrometry techniques still encounter significant challenges, including artifactual features, metabolite annotation, open data, and ethical considerations. Addressing these issues represent the future challenges in this field.

1. Introduction

Metabolites are central to biological function, representing key intermediates in the energy-generating pathways that keep us alive, the building blocks of living cells and viruses, and many of the signals that enable interactions between organisms. Metabolites can be characterized by targeted or untargeted metabolomics. Untargeted metabolomics is conducted without an a priori list of specific metabolites to analyze, usually with the goal of attaining a broad representation of metabolites within a given system. Targeted analyses, in contrast, focus on quantifying metabolites from a predetermined list.

Metabolomics can be performed on bulk extracts, without considering spatial aspects. However, given the central role of metabolites in biological system function, quantifying metabolites is incomplete if the location of a given metabolite is not considered. Infectious diseases are often highly localized, in terms of symptoms and in terms of pathogen colonization sites. Nutrient metabolites that are at insufficient local levels will, for example, prevent pathogen colonization at that location [1]. Deciphering the tissue localization of signaling metabolites can help determine sites and mechanisms of action, for example to elucidate mediators of extra-intestinal effects of the gut microbiota [2]. Local drug accumulation and local drug metabolism are critical concerns in pharmacokinetics, without which a complete understanding of treatment failure vs success is impossible [3]. Metabolite segregation between cellular compartments is a key regulatory aspect enabling metabolic reaction directionality [4]. All these aspects would be missed through conventional analysis of single biofluids or of a single tissue segment, since they do not allow for spatial comparisons. Thus, there is a strong need for spatial metabolomics approaches, which will furthermore help enable a spatial framework for personalized/precision medicine initiatives. Here, we review mass spectrometry-based spatial metabolomics methods, with a focus on their applications in a biomedical context and on future trends in the field.

2. Spatial metabolomics methods

Mass spectrometry (MS)-based spatial metabolomics methods enable metabolite analysis from the sub-micrometer to the meter scale or larger (e.g. Refs. [5–12]. A common aspect across methods is the need to carefully plan sample preparation, followed by data acquisition and data processing to generate spatial metabolite maps (Fig. 1). Among the most

* Corresponding author. Department of Chemistry and Biochemistry, San Diego State University, 5500 Campanile Drive, San Diego, CA 92182, USA.
E-mail address: lmccall@sdsu.edu (L.-I. McCall).
[1] authors contributed equally.

https://doi.org/10.1016/j.trac.2024.117713
Received 6 October 2022; Received in revised form 12 April 2024; Accepted 15 April 2024
Available online 18 April 2024

Abbreviations

3D	three-dimensional
AA	arachidonic acid
DESI	desorption electrospray ionization
FAIR data	findable accessible interoperable and reusable data
FISH	fluorescence in situ hybridization
GC	gas chromatography
GCIB	gas cluster ion beam
GNPS	Global Natural Products Social Molecular Networking
ICP	inductively coupled plasma
LC	liquid chromatography
LPA	lysophosphatidic acid
PE	phosphatidylethanolamine
PI	phosphatidylinositol
MALDI	matrix-assisted laser desorption/ionization
MS	mass spectrometry
MSI	mass spectrometry imaging
NMR	nuclear magnetic resonance
PC	phosphatidylcholine
PET	positron emission tomography
PS	phosphatidylserine
SEAM	spatial single nuclear metabolomics
SIMS	secondary ion mass spectrometry
ToF	time of flight
TIC	total ion chromatogram
TIMS	trapped ion mobility spectrometry
XIC	extracted ion chromatogram

common methods are matrix-assisted laser desorption/ionization (MALDI) mass spectrometry imaging (MSI), secondary ion mass spectrometry (SIMS) and desorption electrospray ionization (DESI) MSI. Another emerging technique is the Single-probe MSI, which can be used to perform single-cell as well as tissue analysis (Fig. 1A).

2.1. Sample selection and preparation

Planning of sample collection and sample preparation to preserve spatial information is the key step without which quality data cannot be obtained. Simple analyses of the impact of location on the cell metabolome can be performed via analysis of cell culture systems, for example in mixed cell culture populations (*e.g.* Ref. [14]) or comparing between infected and infection-adjacent cells following *in vitro* infection [15]. Alternatively, single-cell MS and spatial analysis can be combined by systematically dissociating different regions of a tissue and keeping the resulting cells separated by tissue regions. More commonly, tissue sections are used for spatial metabolomic analysis, preserving more detailed spatial context than analyses of *in vitro* cultured cells or cells dissociated from biological systems. With skilled sectioning, even whole vertebrate sections can be analyzed (*e.g.* Ref. [16]). Greater spatial scales (across a given organ or multiple organs) or comparison between

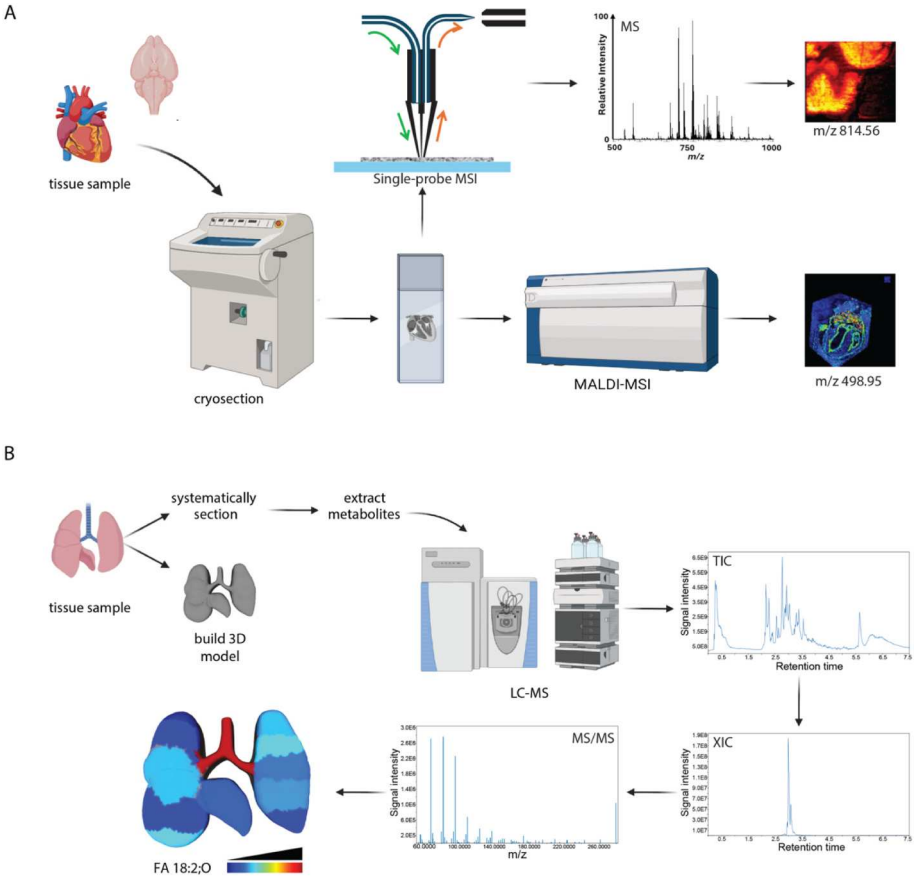

Fig. 1. Representative spatial metabolomics workflows. (A) Workflows based on thin tissue sectioning. Top, single-probe MSI with representative resulting MS spectrum. Bottom, MALDI MSI. (B) Large-scale spatial analyses by LC-MS ("chemical cartography") with representative total ion chromatogram (TIC), extracted ion chromatogram (XIC) and MS/MS spectrum for the corresponding feature, annotated as FA 18:2; O. Figure created using BioRender.com, Adobe Illustrator, and 'ili software [13].

multiple replicates can also be achieved by carefully planned systematic sample sectioning, followed by metabolite extraction, liquid chromatography (LC)-MS analysis on each extract, and computational data reconstructions, an approach termed "chemical cartography" or "molecular cartography" [17] (Fig. 1B). Spatial resolutions of ~1 mm^3 can be achieved using fine swab-based sampling or fine sectioning, though this method is more commonly applied for large-scale spatial analyses. On the other end of the spatial scale, spatial mass spectrometry approaches are also being applied to individual organelles and to elucidate subcellular metabolite distribution [9,18].

In all cases, careful and appropriate sample preparation methods are critical. They should limit metabolite degradation, preserve metabolite sample distribution (for example by avoiding diffusion or delocalization of metabolites) and preserve overall tissue biogeography or integrate sufficient reference points to enable correction of sample distortion introduced for example during desiccation of tissue slices [19]. Choices, such as fixation, matrix selection, desorption solvent, metabolite extraction solvent, data acquisition instrument and data acquisition polarity, will all determine the metabolite classes that can be detected in a given spatial metabolomics experiment [20,21]. While broad metabolite coverage is often the goal, full and complete metabolite coverage is not currently possible and often only a small fraction of the metabolites in a given sample are detectable and detected. The detectable metabolite classes will depend on the sample preparation and mass spectrometry techniques selected.

2.2. Data acquisition approaches

2.2.1. Vacuum-based methods

In SIMS, a primary ion beam is applied to the sample surface, leading to the generation and ejection of secondary ions from the sample, which are then separated in a mass analyzer. Spatial data is acquired by systematically moving the ion beam across the sample surface, with lateral spatial resolution in the nanometer to micrometer range, a strength compared to most other alternative approaches. SIMS can also generate three-dimensional (3D) molecular maps as the sample surface is progressively eroded. There are multiple types of SIMS instrumentation, with various primary ion beams, lens positioning and mass analyzers, depending on the desired lateral and depth spatial resolution, speed of data acquisition, mass resolution and mass accuracy [9,22,23]. SIMS was originally predominantly restricted to elemental analysis and metabolites that are non-volatile under ultra-high vacuum; data analysis can also be hampered by the fragmentation induced by the ion beam. However, instrumental developments, such as Cryo-OrbiSIMS or new ion beam technologies, such as GCIB, expand these limits [22,24].

MALDI is another method that is most commonly vacuum-based, in which analytes are co-crystallized with a small molecule matrix. This matrix absorbs energy from a laser beam rastered along a surface, leading to desorption and ionization of the matrix and analytes, generally in protonated or deprotonated forms. The chemical properties of detectable analytes are strongly influenced by matrix choice, with new matrices expanding the ranges of metabolites that can be detected by MALDI-MSI (*e.g.* Ref. [20]; see Ref. [25] for a comprehensive review). MALDI has a wider spatial resolution than SIMS, usually 5–100 μm, though finer lateral resolutions can be achieved with modifications such as atmospheric pressure MALDI and improved sample preparation procedures [26]. 3D maps can also be generated with MALDI, though it is more difficult than via SIMS due to the need for data acquisition and integration across multiple tissue segments (e.g. Ref. [27]). Although vacuum-based techniques provide very high spatial resolution and sensitivity, complex sample preparation is generally required. In addition, matrix application and high-vacuum working environments can potentially alter the samples.

2.2.2. Ambient methods

Ambient MSI techniques were designed to overcome the intrinsic drawbacks of vacuum-based methods. DESI was the first ambient-based MS technique developed for surface analysis [28]. This technique rasters charged solvent droplets onto a sample to desorb sample analytes from the sample surface for direct MS analysis. DESI is classically best suited for polar analytes, though modifications in sample preparation, solvent composition or instrumentation can expand this range [29]. Unlike MALDI-MSI, which requires matrix embedding and usually ionization under vacuum, DESI-MSI requires no sample preparation and can be done at room temperature and atmospheric pressure, which allows quick analysis of spatially distributed molecular information. Disadvantages include a lower spatial resolution compared to SIMS or MALDI. However, recent technology development of DESI significantly improved its spatial resolution to 20 μm [30].

Other ambient MSI techniques have been reported with improved spatial resolution. Despite the similarity of their names, the working mechanisms of DESI and nano-DESI are fairly different. Nano-DESI produces microscale liquid to extract analytes on the sample surface for real-time MS analysis with a spatial resolution better than 12 μm [31]. The Single-probe, which has a similar working mechanism as nano-DESI, is fabricated by integrating one dual-bore quartz needle, one solvent-providing capillary, and one nano-electrospray ionization (nano-ESI) emitter. The sampling liquid (e.g., methanol and acetonitrile) is continuously delivered through the solvent-providing capillary via a syringe pump. A small liquid junction, which is formed at the tip of the dual-bore quartz needle, contacts the tissue surface to dissolve analytes present on a small spot of the tissue. The extracted molecules are then automatically drawn (via a self-aspiration process) towards the integrated nanoESI emitter for real-time MS detection. This technique has been primarily used for imaging small molecules, such as metabolites, lipids, and drug compounds on animal tissues, and a high spatial resolution of ca. 8.5 μm can be achieved [32] (Fig. 1A). Both the nano-DESI and Single-probe are not commercially available, and the device fabrication and experiment operation require extensive experience. However, these methods have been adopted by other research groups, facilitating technology advancement and more applications [33–36].

3. Representative applications in health

Spatial metabolomics can provide considerable insight into the role of location in healthy organ function as well as disease processes (Fig. 2). We illustrate the former by highlighting spatial metabolomics applications in the context of brain physiology and microbiome-host communication. The brain was selected because its inherent spatial architecture makes it one of the most common and earliest organs selected to test novel MSI techniques (e.g. Ref. [37]). Spatial metabolomics applications to the study of the microbiome are newer. The microbiome produces a considerable diversity of small molecules, with local as well as far-ranging effects that necessitate a spatial approach [38].

3.1. Understanding the brain

Given the brain's distinct architecture, it has commonly been used as a biological system to validate and illustrate the strengths of novel spatial metabolomic techniques. For example, the original publication on 3D OrbiSIMS used this technique to reveal the fine spatial distribution of cholesterol and phosphoinositides in the mouse hippocampus, adenine accumulation at the single nucleus level, and γ-aminobutyric acid neurotransmitter accumulation in the stratum oriens region [9]. Likewise, water GCIB-SIMS was implemented to show differential abundance of specific sulfatides, phosphatidylinositols, glutathione, adenosine monophosphate, and fatty acids between the outer layer of the cerebellum cortex, the middle layer, the granular layer and the white matter in mice [39].

Beyond these demonstrations of instrumentation capabilities, spatial metabolomics techniques have been implemented to provide functional insight into brain physiology. Specifically, major challenges in our

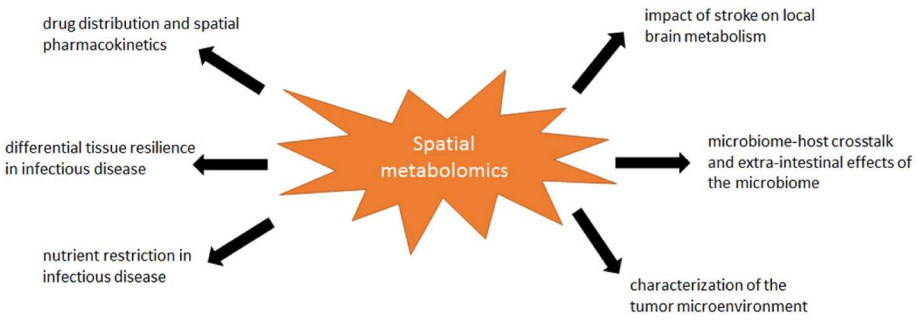

Fig. 2. Example applications of spatial metabolomics.

understanding of the brain include mapping the relationship between chemical signaling, brain anatomical structures and brain function, and differentiating between healthy aging-associated changes vs pathological alterations. For example, Ding et al. used tissue sectioning followed by metabolite extraction and LC or gas chromatography (GC)-MS to compare the regiospecific brain metabolome between ages and sexes in mice. Results showed a dominant effect of age over sex, including different patterns of sphingolipid species abundance, providing a chemical mechanism underlying myelin degeneration. Furthermore, regions with similar function showed similar metabolism, providing an important link between chemistry and physiology [40].

3.2. *Understanding the microbiota*

The mammalian microbiota, the community of microorganisms living on and in a mammalian body, is restricted to specific colonization sites. However, studies in germ-free and antibiotic-treated mice have revealed far-ranging effects of the microbiota in organs distal to sites of microbiota colonization [41]. Spatial metabolomic approaches can be used to identify the metabolite mediators and metabolic consequences of these far-ranging effects. For example, a systematic "chemical cartography" comparison of tissue metabolite levels across organ segments, in germ-free vs colonized mice, identified novel microbiota-produced bile acid conjugate molecules: phenylalanocholic acid, tyrosocholic acid and leucocholic acid. These metabolites were found predominantly in the ileum, duodenum, and jejunum of colonized mice, while there was a ten-fold decrease in detection of the same conjugated bile acids in the caecum and colon [42].

On a finer spatial scale, MALDI-MSI and DESI-MSI revealed higher levels in the white matter of colonized mice compared to brains from germ-free mice, of a mixture of 3-methyl-4-(trimethylammonio)butanoate and 4-(trimethylammonio)pentanoate, which inhibited fatty acid oxidation, thus expanding our understanding of the gut-brain axis [43]. However, deconvoluting microbiota vs host origin is challenging for metabolites that are potentially produced by both prokaryotes and eukaryotes. To address this issue, Uchimura et al. colonized germ-free mice with ^{13}C or ^{12}C-labeled non-replicating *Escherichia coli* bacteria. Bacterially-derived amino acids reached many organs including the liver, brain, spleen and pancreas within 2 h, with differential abundance depending on the organ and the amino acid [2]. Spatial metabolomics using MALDI-MSI also enabled finer characterization of microbiota metabolism. Specifically, one study found that *B. subtilis* produces the antibiotics surfactin and plipastatin at higher levels near zones of cross-species interaction [44].

However, the integration of metabolomics analysis with microbiome data can be challenging. Limitations in current dissection methods result in the loss of spatial resolution at the level of individual cells [45], and bacterial constituents of the microbiome are at or below the spatial resolution of MALDI-MSI, the most common fine-scale MSI instrumentation available to microbiology laboratories. SIMS studies of microorganisms have either focused on elemental analysis, environmental microorganisms (*e.g.* Refs. [46–48]), or pathogenic microorganisms (e.g. Ref. [23], see below). Additionally, many microbiota metabolites are still of unknown identity. Indeed, this is a particular challenge across metabolomics studies, with considerable signals that cannot currently be annotated, either because they are instrumental artefacts, or because they represent novel chemical matter (especially from microorganisms) [49,50]. Advances in genomic and metabolite databases and new data processing tools will help address the latter issue [51]. An emerging approach is dual MALDI-MSI and fluorescence in situ hybridization (FISH), to identify the specific microbes producing metabolites of interest locally [10]. Improved communication between microbiome researchers and bio-analytical chemists focused on small molecule characterization will enable increased expansion of spatial metabolomic techniques to study the microbiome [52].

4. Representative applications in disease

4.1. *Cancer*

Spatiality is central in cancer pathophysiology and treatment, from defining tumor margins to understanding sites and consequences of metastasis. Indeed, determination of tumor margins during surgery is one of the major clinical applications of spatial metabolomics [53]. Other implementations in a laboratory setting have generated fundamental insight into cancer pathogenesis, for example by characterizing the tumor microenvironment. Using MALDI-MSI, Randall et al. demonstrated high levels of acylcarnitines at the tumor periphery, anti-correlated with ATP [54]. Zink et al. likewise used MALDI-MSI and agarose-embedded cells and ovarian explants to show that ovarian tissue produces norepinephrine in the presence of fallopian tube-derived transformed cells, and that norepinephrine promotes invasiveness of cancer cells [55]. Additional insight can be provided by multi-modal data acquisition. For example, airflow-assisted DESI-MSI showed increased proline levels in esophageal squamous cell carcinoma. Combining this approach with immunohistochemistry demonstrated that the rate-limiting enzyme in proline biosynthesis was likewise upregulated in these tumors, and similar concurrent patterns were observed between metabolites and enzymes in glutamine metabolism [56]. Likewise, protein and metabolite spatial distribution were analyzed in parallel in the human breast cancer tumor microenvironment via SIMS, taking advantage of lanthanide-labeled antibodies. This approach revealed for example higher levels of lysophosphatidic acid LPA (20:0) in highly-proliferative cells (marked by Ki-67 -positive regions) and higher polyunsaturated lipids in infiltrating macrophages [57]. Expanding this approach to other protein markers and other cancer types shows great promise, and may lead to the development of novel therapeutic regimens in oncology.

4.2. *Neurological disorders*

Spatial metabolomics findings on healthy brain function can be

extended in the context of neurological disorders, with emphasis on neurodegenerative diseases, traumatic brain injury, and stroke. For example, MALDI-MSI revealed lower dopamine and norepinephrine in damaged brain regions in rat Parkinson's disease models, and that levodopa treatment led to elevated striatum γ-aminobutyric acid levels [20]. MALDI-MSI also found that gangliosides were overall lower in the cerebellum and right hemisphere in a mouse model of Alzheimer's disease compared to controls. These findings may help expand our understanding of Alzheimer's disease pathogenesis [58].

Likewise, MALDI-MSI studies of mouse brains after experimentally-induced stroke revealed striking spatial metabolomic differences between infarcted vs healthy sites. Glucose and citric acid were elevated whereas guanosine monophosphate (GMP), adenosine diphosphate (ADP), inosine carnitine, glutathione and $[PC(32:0) + K]^+$ were decreased [59,60]. This may reflect metabolic shifts in response to limited oxygen availability, as well as inability to protect against oxidative damage. Importantly, these manuscripts also used a spatial approach to test whether new therapeutics could improve this aberrant distribution [60,61].

In the context of traumatic brain injury, GCIB-SIMS revealed significant loss of polyunsaturated cardiolipin in the ipsilateral contusional cortex and CA3 region of the brain hippocampus in rats. The CA3 region plays a role in memory, so loss of cardiolipin in this region could explain poor cognitive performance after head injury [22]. In another rat study, GCIB-SIMS showed selective accumulation of specific phosphatidylethanolamine PE (38:4)-OH and arachidonic acid AA (20:4)-OH oxidized lipids in the ipsilateral pericontusional cortex, with concomitant loss of the non-oxidized phosphatidylethanolamine and accumulation of free fatty acids [62]. 3D MALDI-MSI further revealed elevated phosphatidylcholine PC(42:9) at the lesion site in rats [63]. As with the analyses of stroke, above, MALDI-MSI was also used to characterize the spatial response to treatment, revealing a decrease in specific ceramide at the impact site in animals treated with a "decoy" peptide [64]. Thus, spatial metabolomics analyses can not only provide insight into the pathogenesis of neurological damage, but also assess treatment efficacy.

4.3. Infectious disease

4.3.1. Bacterial infection

Infection is often a location-specific process: pathogens accumulate at specific body sites, and symptoms may manifest in discrete locations. In the context of bacterial infection, MALDI-MSI was used to track the virulence factor lipid A in the mouse spleen during *Francisella novicida* infection, in comparison with time-dependent spatial loss of phosphatidylinositol (PI) 18:0/20:4. *F. novicida* serves as a model for *Francisella tularensis* ssp. *tularensis*, causative agent of tularemia. PI(18:0/20:4) is a precursor of inflammatory lipids such as arachidonic acid. These findings are helping to define the role of arachidonic acid and cyclooxygenase-2–dependent inflammation in tularemia [65]. Likewise, bacteria and the host compete for iron in tissue abscesses caused by *Staphylococcus aureus*. Tracking siderophores by MALDI-MSI and iron by inductively coupled plasma (ICP)-MS in parallel showed the uneven distribution of iron availability vs uptake in the tissue abscesses collected from mouse liver, kidney, and heart [66]. Additional MALDI-MSI analyses of samples from murine and human *S. aureus* infection revealed variable lysyl-phosphatidylglycerol lipid levels between infection foci. This may indicate heterogenous bacterial response to a common host environment, or underlying variation in the host environment leading to differential bacterial virulence factor expression [67]. Similarly, multiple separate studies used time of flight (ToF)-SIMS to analyze *Pseudomonas aeruginosa* biofilms, demonstrating spatial heterogeneity of quinolone specialized metabolites and accumulation of quinolones around the perimeter of bronchial sections [23,68].

MALDI-MSI is also useful to study the distribution of host molecules involved in infectious diseases. For example, bile acid access is crucial to bacterial infection by *C. difficile*. MALDI-MSI revealed elevated levels of the bile acid taurocholate in the ileum of *C. difficile*-infected mice [69]. Similarly, analysis of mouse liver infection by *S.* Typhimurium using DESI-MSI and immunohistochemistry revealed co-localization of neutrophils, dendritic cells, monocytes and macrophages with phosphatidylcholine-plasmalogens and long-chain acylcarnitines. These findings provide insight into immunometabolic changes during *Salmonella* infection [70].

In addition to these microscale analyses, broader-scale chemical cartography workflows can also provide significant insight into bacterial infection. A chemical cartography study of the lung of a cystic fibrosis patient revealed a disconnect between homogenous *Pseudomonas aeruginosa* spatial distribution and patchy production of its quinolone and rhamnolipid virulence factors across the lung [17]. This heterogenous virulence factor production may reflect differential contact with other, heterogeneously-distributed bacteria in the lung [71]. Another pathogen which is associated with cystic fibrosis, *Achromobacter*, was negatively correlated with the antibiotic meropenem [17]. This approach may help understand *in vivo* resistance to antimicrobial agents.

To enable application of these methods to highly pathogenic agents, pathogen inactivation methods compatible with spatial metabolomics need to be developed and optimized. Chemical cartography is at an advantage here, as many standard metabolite extraction solvents will inactivate pathogens (*e.g.* dichloromethane; methanol). With regards to other spatial metabolomics approaches, method validation is necessary. Wang et al. recently demonstrated that 100°C heat killed *Mycobacterium tuberculosis* and was compatible with lipid analysis by MALDI-MSI. The authors showed that different sphingomyelin species accumulate in cellular lesion regions, caseous lesion regions, and adjacent undamaged lung tissue, as well as variability between lesions [21]. Other methods such as short glutaraldehyde fixation may also be suitable for such studies [15].

4.3.2. Parasitic infection

Parasitic infections are neglected compared to many bacterial infections and thus there have been fewer applications of spatial metabolomics to study parasitic diseases. These diseases are poorly understood and would benefit from the insights enabled by these technologies. Indeed, when these techniques were applied to Chagas disease, they provided the first mechanistic explanation for the localization of Chagas disease symptoms in the body and a novel mechanism of disease tolerance. Chagas disease is caused by the parasite *Trypanosoma cruzi,* and in chronic cases causes enlargement of the heart, esophagus and colon. Chemical cartography analyses of the *T. cruzi*-infected heart and gastrointestinal tract in mouse models showed persistent metabolic perturbations specifically at these sites of symptom localization and disconnected from parasite load. In addition, results revealed local perturbation of acylcarnitines and glycerophosphocholines during infection with different *T. cruzi* strains and in accordance with disease severity. Modulating carnitine levels induced tolerance to *T. cruzi* infection via restoration of the cardiac metabolome and lowered cardiac strain in mice [72–74]. MALDI-MSI in combination with autofluorescence microscopy enabled detection of *Plasmodium*-infected cells in the mouse liver, which had high localized levels of phosphatidylserine PS(40:5) [75]. This method could help understand the local metabolic changes associated with *Plasmodium* liver infection, which would be missed by bulk tissue analyses due to the low parasite load.

4.4. Drug distribution

Spatial metabolomics approaches have often been used to investigate drug distribution. Indeed, poor drug bioavailability and pharmacokinetics are a major cause of drug failure during drug development. Drug efficacy and drug safety are thus dependent on drug tissue distribution.

Eye drops are commonly used for a variety of eye conditions. Some chemical constituents of eye drops are toxic to parts of the eye, like benzalkonium chloride [76]. Other common issues with eye drops are

Table 1
Frontiers in spatial metabolomics.

Challenge	Examples
Instrumentation	• Spatial resolution • Spatial co-registration • Sensitivity and matrix effect • Structural coverage • Absolute quantification • MS^n • Ease of use and learning curve for new users • Data size and complexity • Molecular information extraction
Annotation	• Quality MS/MS data • Differentiating between metabolites and artefacts/contaminants • Spectral library breadth • *In silico* structure prediction and annotation confidence
Multi-omics	• Diversity of metabolite identifiers • Differential nomenclature across data types • Integration of multi-omics data
Ethics	• FAIR data principles • Accessibility • Privacy
Translational implementation	• Clinical use • Impact on drug development • Disconnect between analytical chemists and biologists

the constituents not reaching the correct part of the eye for treatment, such as atropine which must reach the sclera [77]. ToF-SIMS and MALDI-MSI were used to characterize the spatial distribution of these constituents and their local concentrations in rabbit models [76–78].

Studying the distribution of drugs in diseased tissues is important to ensure that the drug is concentrated enough in the correct area to properly treat the infection. In the case of leishmaniasis, miltefosine decreases the parasite load, but the disease often recurs in patients who were thought to be cured. MALDI-MSI showed that miltefosine was unable to reach parasites lying dormant in collagen-rich lesional tissues in a mouse model of cutaneous leishmaniasis [3]. Likewise, in tuberculosis, emergence of drug resistance has been tied to tuberculosis granulomas not allowing full drug penetration. Specifically, moxifloxacin, an anti-tuberculosis drug, was found by MALDI-MSI to accumulate at the granuloma edge rather than core, indicating incomplete drug penetration in a rabbit model of disease [79]. Chemical cartography approaches likewise revealed heterogenous drug distribution throughout the lung of cystic fibrosis patients for three different drugs (meropenem, piperacillin and ciprofloxacin), and found that azithromycin was the only drug to uniformly penetrate the lung [17]. Similarly, in cancer, MALDI-MSI revealed a zone with low erlotinib levels at the tumor periphery, maybe due to pH gradients affecting erlotinib solubility [54]. For multicellular pathogens, drug distribution within the pathogen is also important for drug efficacy. Using atmospheric-pressure scanning microprobe MALDI MSI, oral uptake of imatinib was observed in the esophagus of male and female *Schistosoma mansoni* [80].

These techniques can also be used to study drug adverse effects. For example, a particular HIV treatment involves the combinations of emtricitabine (FTC), tenofovir (TFV), efavirenz (EFV), or rilpivirine (RPV). After treatment using either the TFV–FTC–EFV combination or the TFV–FTC–RPV combination in mice, MALDI MSI was used to investigate drug accumulation in the kidneys, liver and brain, which could cause organ toxicity [81]. Overall, these approaches can help understand drug treatment success and mechanisms associated with treatment failure.

5. Frontiers in spatial metabolomics research

Novel data acquisition approaches and data analysis tools are constantly being developed to enable increasingly finer spatial resolution (*e.g.* Refs. [9,82,83]), though the utility of large-scale spatial analyses should not be ignored either (*e.g.* Ref. [42]). Approaches are also being developed to analyze a broader range of metabolites (*e.g.* Ref. [24]), though metabolite feature annotation remains a challenge. Likewise, improved data analysis approaches are also needed, including multi-omics methods. In all cases, there is a need for compliance with findable, accessible, interoperable and reusable ("FAIR data") open data principles (Table 1).

5.1. New emerging analytical and instrumental approaches

New approaches with finer spatial resolution are enabling characterization of subcellular organellar metabolomes. One example of an emerging approach is SEAM (spatial single nuclear metabolomics), which combines ToF-SIMS with improved computational algorithms, enabling demarcation of individual cell nuclei and demonstrating one specific hepatocyte subtype that is more abundant near sites of liver fibrosis [83]. Likewise, 3D OrbiSIMS revealed subcellular sites of accumulation of the drug amiodarone in single macrophages [9]. Another SIMS study demonstrated focal accumulation of purine biosynthesis intermediates, providing the first functional evidence of an active metabolon (complex of sequential enzymes in a given metabolic pathway) [82].

One challenge with analysis of increasingly fine spatial resolution is reduced ion abundance. One new method addresses this issue through laser-induced post-ionization in a transmission mode MALDI-MSI set-up ("MALDI-2"), broadening the range of ionizable and detectable metabolites [84]. Detection limits have also been improved by new reactive MALDI matrices [20]. Combining ion mobility with current spatial metabolomics workflows, such as MALDI, nano-DESI, and liquid extraction surface analysis (LESA), can provide greater annotation confidence and help increase sensitivity [16,85–87]. However, adding this additional measurement dimension will increase dataset size, already a challenge in spatial metabolomic studies. Likewise, some of the current data analysis software may not currently be able to handle ion mobility data, thus leading to data processing challenges.

5.2. Annotation confidence

Although spatial metabolomics can be performed in a targeted fashion, especially when using LC-MS [7], it is most commonly performed through untargeted acquisition approaches, unlike other technologies such as microscopy which focus on known signals. Metabolite

annotation is a recurrent challenge in untargeted metabolomics in general. Usually less than 30 % of signals can be annotated in a given study [88]. New computational tools for metabolite annotation (*e.g.* Ref. [89]) will also benefit spatial metabolomics. Methods that can calculate false discovery rates are being developed for metabolomics in general and spatial metabolomics in particular [90]. However, expanded implementation of these and complementary methods by researchers in the field is necessary. A further limitation is that many MSI studies still rely solely on MS1 for compound annotation, leading to an inability to differentiate between isomers. To address this issue, Ellis et al. used full-scan Fourier transform mass spectrometry data acquisition to guide data-dependent MS2 acquisition at an adjacent imaging position via ion trap MS2, using an LTQ Orbitrap Elite instrument coupled to their MALDI source [91]. Adding ion mobility dimensions is also proving highly effective at enabling differentiation of isomers. These novel instruments confirm that isomers are a highly prevalent problem in spatial metabolomics, with 29 % of the most abundant *m/z* values representing multiple species by ion mobility in one study [16]. Combining trapped ion mobility spectrometry (TIMS) with spatial distribution analysis by MALDI, for example, revealed that a detected *m/z* 848.55 feature was a combination of two unique mobility ranges, one of which had the same spatial distribution as $[PC(38:5) + K]^+$, thus differentiating this *m/z* 848.55 feature into $[PC(38:4) + K]^+$ and the M + 2 peak of $[PC(38:5) + K]^+$ [85]. Ion mobility has also been coupled to nano-DESI or liquid extraction surface analysis MSI [92]. Expanded generation of standard measurements and ion mobility libraries is essential to enable ion mobility-supported metabolite annotation [93]. Broader implementation of this technique will be facilitated by the fact that combined MALDI-ion mobility instruments are now commercially available [94].

5.3. Methods that minimize artefacts and increase robustness

Great care in sample preparation and data acquisition are critical, as these are the steps that determine downstream data quality. As with any analytical approach, it is essential to ensure that the methods employed do not introduce any artefacts. For example, the process of cell sorting can affect most metabolite classes [95]. For swab-based chemical cartography approaches, polymer swabs can lead to ion suppression and should thus be avoided in favor of cotton swabs [13]. Pathogen inactivation techniques should be validated to demonstrate that they only minimally affect the chemical profile. As an example, the heat-inactivation method developed by Wang et al. for *Mycobacterium tuberculosis* was only suitable for lipids [21]. Duration of storage and storage temperature also impact the (spatial) metabolite profile [19]. Combining stable isotope labeling with MSI can help demonstrate that detected features represent true metabolic products, rather than artefacts caused by laser irradiation during the ionization process in MALDI-MSI, for example [96]. In experiments using electrospray ionization and in most workflows that lack a chromatography step, ion suppression effects and differential ionization efficiencies should also be kept in mind [97]. A further issue is the need for data acquisition methods that incorporate sufficient reproducibility and speed of analysis to enable comparison between multiple replicate samples. LC-MS/MS based chemical cartography approaches can readily analyze sufficient replicates to enable statistical analyses (*e.g* Refs. [72,73]). New data analysis tools have also recently been developed to assess and improve the reproducibility of metabolomics and spatial metabolomics data (*e.g.* Refs. [98,99]).

5.4. Multi-omics and data integration

Spatial metabolomics requires integration with external data types such as histological section images or magnetic resonance imaging (MRI) data (e.g. Refs. [42,54]). Integrating microscopic images with MSI data may be challenging if the staining process distorts the sample differentially from the sections used for MSI experiments. Data integration may also be desirable between two different spatial metabolomics techniques, for example differing in spatial resolution and data acquisition speed. Race et al. have addressed this issue by developing a new algorithm that can fuse MALDI-MSI and SIMS data [100]. One alternative to address co-registration issues is to acquire multimodal data from the same sample, for example by combining spatial analysis of metabolites and lipids with analysis of metal-tagged antibodies to differentiate between cell types using SIMS [57]. Correlation between 'omics datasets is also of great interest. Indeed, integration of the many spatial transcriptomic approaches with spatial metabolomics may be a particularly rich source of biological insight [83]. However, a challenge to doing so is the use of multiple different styles and names to describe the same metabolite. This is being partially addressed by tools such as RefMet [101] and LipidMaps standardized lipid nomenclature [102]. All multi-omics correlations should also consider data sparsity and compositionality (e.g. Ref. [103]).

5.5. New visualization approaches

Visualizing what is inherently 3D data in the two dimensions of a manuscript page is inherently reductionist. Video figures and supplementary data can help bridge that gap, as can embedded 3D figures in pdf files [104]. Augmented and virtual reality approaches are the next logical step and are beginning to be implemented [105–107]. These currently benefit from the broad availability of smartphones and the increasing availability and affordability of virtual reality headsets.

5.6. Open data, FAIR principles and ethical considerations

Generating spatial metabolomics data that is FAIR (findable, accessible, interoperable and reusable) benefits the broader scientific community, by enabling external evaluation and validation of findings and to serve as the foundation for new research avenues. Some of these goals can be achieved by depositing spatial metabolomics data into existing repositories such as MassIVE/GNPS (Global Natural Products Social Molecular Networking [108]), the Metabolomics Workbench [109] and MetaboLights [110]. There are also databases specific to MSI data such as METASPACE [90]. Such databases are especially critical, since spatial metabolomics datasets are usually much larger than non-spatially resolved biofluid analyses, for example, especially if multiple replicate samples are included in the spatial analysis. However, these open data practices must also consider participant privacy and the protection of study subjects [111].

Inter-operability in spatial metabolomics is also often challenging. In particular, feature peak areas obtained on different instruments and by different laboratories may be difficult to compare unless absolute quantification is performed. Purpose-built and novel instrumentation are often restricted to the research group that designed them. Likewise, proprietary software or in-house code that is not shared restrict accessibility and reproducibility of spatial metabolomics analyses. One possible solution is the implementation of open spatial metabolomics quality control and data processing tools within the Galaxy framework [112], in combination with publisher mandates similar to those for genetic sequencing information. Detailed methods in scientific publications are critical, complying with the guidelines of the Metabolomics Standards Initiative [113] and mass spectrometry imaging-specific guidelines such as MSIcheck [114,115]. Lastly, even though costs for spatial metabolomics analyses are often greater than traditional biofluid metabolomic analyses, it will be important to ensure that everyone benefits from the generated insights, including people suffering from rare or neglected diseases.

5.7. Translational frontiers

5.7.1. Clinical implementation

Determining metabolite localization can provide valuable insight into metabolite function in health and disease. However, invasive biopsy collection, even when feasible, is certainly less desirable from a patient perspective. Thus, from a diagnostic perspective, it is necessary to assess whether the metabolic changes observed at sites of tissue damage can be quantified in biofluids or by non-invasive positron emission tomography (PET) scan approaches. There are multiple available PET tracers that can assess carbohydrate metabolism, fatty acid metabolism and amino acid metabolism [116,117], or even antibiotic uptake by bacteria *in vivo* [118].

In a surgical context, spatial metabolomics analyses are already being implemented to determine tumor margins, for example with the iKnife (rapid evaporative ionization mass spectrometry (REIMS)) [119,120], the MassSpec Pen (water-based extraction followed by electrospray ionization and MS) [121,122] or using DESI-MS [123]. Broader implementation will need to consider cost and ease of use and training, building on these demonstrations of feasibility. This may be facilitated by recent advances such as the integration of the MassSpec Pen into standard surgical robotics systems [53]. A further necessary consideration will be cross-site reproducibility, especially with regards to prediction accuracy, once these techniques expand beyond the developers' laboratories [99].

5.7.2. Drug development

Spatial metabolomics approaches have been extensively implemented to study drug distribution and drug metabolism [124,125]. However, most of these studies have been performed in healthy animals, with some exceptions (*e.g.* Ref. [3]). Having observed that drug distribution can differ between infected and healthy tissue [74], it will be necessary to focus future drug distribution and metabolism studies on disease models. Spatial analyses of microbe-microbe or microbe-host interactions are also being used to discover new antibiotics (*e.g.* Ref. [126]), drug mechanisms of action (*e.g.* Ref. [127]), or host-targeted treatments [69,73]. As an example, MALDI-MSI-derived insights into the relationship between bile acid distribution and *C. difficile* bacterial infection led to the development of an experimental cholestyramine-based treatment strategy tested in mice [69]. One challenge, however, is that follow-through from spatial metabolomic discoveries to drug development is often lacking, likely due to the differential expertise and interests involved.

6. Discussion and conclusion

This review focused on MS-based approaches for spatial metabolomics. Spatial mass spectrometry analysis has been increasing in the past 25 years. Initially dominated by MALDI-MSI, there is now increasing implementation of DESI-MSI, as well as combination with ion mobility. Beyond the scope of this review, there are also many exciting spatial methods involving other analytical methods such as spatial nuclear magnetic resonance (NMR) spectroscopy (*e.g.* Ref. [128]), Raman spectroscopy (*e.g.* Ref. [129]), and PET (*e.g.* Ref. [116]). New MS-based techniques for spatial metabolomics and spatial metabolomics data analysis are also constantly being developed (*e.g* Refs. [14,57,83]). Overall, including a spatial aspect to metabolomics analyses grants a new level of understanding of the role of metabolism in disease pathogenesis, lending itself to more effective diagnostic, prevention, and treatment methods in a spatial precision medicine framework.

CRediT authorship contribution statement

Kate Wheeler: Writing – original draft. **Camil Gosmanov:** Writing – original draft. **Michael Jimenez Sandoval:** Writing – original draft. **Zhibo Yang:** Formal analysis, Funding acquisition, Writing – original draft, Writing – review & editing, Visualization. **Laura-Isobel McCall:** Conceptualization, Formal analysis, Funding acquisition, Investigation, Project administration, Supervision, Visualization, Writing – original draft, Writing – review & editing.

Declaration of competing interest

The authors declare that they have no known competing financial interests or personal relationships that could have appeared to influence the work reported in this paper.

Data availability

No data was used for the research described in the article.

Acknowledgements

The study of metabolism and infection in the McCall laboratory is supported by the National Institute of Allergy and Infectious Diseases of the National Institutes of Health under awards number R01AI168038, R01AI170605 and by the National Science Foundation (NSF), award number 2344946. Laura-Isobel McCall, Ph.D. holds an Investigators in the Pathogenesis of Infectious Disease Award from the Burroughs Wellcome Fund. Zhibo Yang is supported by the National Science Foundation (NSF) CMI-2305182 and the Research Council of the University of Oklahoma Norman Campus. Zhibo Yang and Laura-Isobel McCall jointly received research support through the Chan Zuckerberg Initiative DAF and NIAID award number R01AI177469. The content is solely the responsibility of the authors and does not necessarily represent the official views of the funders. We wish to thank the authors of the exciting work we reviewed here, and to apologize to those whose work we could not cover due to space limitations.

References

[1] L.-I. McCall, Quo vadis? Central rules of pathogen and disease tropism, Front. Cell. Infect. Microbiol. 11 (2021), https://doi.org/10.3389/fcimb.2021.640987.
[2] Y. Uchimura, T. Fuhrer, H. Li, M.A. Lawson, M. Zimmermann, B. Yilmaz, J. Zindel, F. Ronchi, M. Sorribas, S. Hapfelmeier, S.C. Ganal-Vonarburg, M. Gomez de Agüero, K.D. McCoy, U. Sauer, A.J. Macpherson, Antibodies set boundaries limiting microbial metabolite penetration and the resultant mammalian host response, Immunity 49 (2018) 545–559.e5.
[3] J. Kloehn, B.A. Boughton, E.C. Saunders, S. O'Callaghan, K.J. Binger, M. J. McConville, Identification of metabolically quiescent leishmania mexicana parasites in peripheral and cured dermal granulomas using stable isotope tracing imaging mass spectrometry, mBio 12 (2021), https://doi.org/10.1128/mbio.00129-21.
[4] W. Quiñones, H. Acosta, C.S. Gonçalves, M.C.M. Motta, M. Gualdrón-López, P.A. M. Michels, Structure, properties, and function of glycosomes in trypanosoma cruzi, Front. Cell. Infect. Microbiol. 10 (2020), https://doi.org/10.3389/fcimb.2020.00025.
[5] D. Petras, L.-F. Nothias, R.A. Quinn, T. Alexandrov, N. Bandeira, A. Bouslimani, G. Castro-Falcón, L. Chen, T. Dang, D.J. Floros, V. Hook, N. Garg, N. Hoffner, Y. Jiang, C.A. Kapono, I. Koester, R. Knight, C.A. Leber, T.-J. Ling, T. Luzzatto-Knaan, L.-I. McCall, A.P. McGrath, M.J. Meehan, J.K. Merritt, R.H. Mills, J. Morton, S. Podvin, I. Protsyuk, T. Purdy, K. Satterfield, S. Searles, S. Shah, S. Shires, D. Steffen, M. White, J. Todoric, R. Tuttle, A. Wojnicz, V. Sapp, F. Vargas, J. Yang, C. Zhang, P.C. Dorrestein, Mass spectrometry-based visualization of molecules associated with human habitats, Anal. Chem. 88 (2016) 10775–10784.
[6] L.-I. McCall, V.M. Anderson, R.S. Fogle, J.J. Haffner, E. Hossain, R. Liu, A.H. Ly, H. Ma, M. Nadeem, S. Yao, Analysis of university workplace building surfaces reveals usage-specific chemical signatures, Build. Environ. 162 (2019) 106289, https://doi.org/10.1016/j.buildenv.2019.106289.
[7] M. Katemauswa, E. Hossain, Z. Liu, M. Lesani, A.R. Parab, D.A. Dean, L.-I. McCall, Enabling quantitative analysis of surface small molecules for exposomics and behavioral studies, J. Am. Soc. Mass Spectrom. 33 (2022) 412–419.
[8] D. Petras, J.J. Minich, L.B. Cancelada, R.R. Torres, E. Kunselman, M. Wang, M. E. White, E.E. Allen, K.A. Prather, L.I. Aluwihare, P.C. Dorrestein, Non-targeted tandem mass spectrometry enables the visualization of organic matter chemotype shifts in coastal seawater, Chemosphere 271 (2021) 129450.
[9] M.K. Passarelli, A. Pirkl, R. Moellers, D. Grinfeld, F. Kollmer, R. Havelund, C. F. Newman, P.S. Marshall, H. Arlinghaus, M.R. Alexander, A. West, S. Horning, E. Niehuis, A. Makarov, C.T. Dollery, I.S. Gilmore, The 3D OrbiSIMS-label-free

metabolic imaging with subcellular lateral resolution and high mass-resolving power, Nat. Methods 14 (2017) 1175–1183.
[10] B. Geier, E.M. Sogin, D. Michellod, M. Janda, M. Kompauer, B. Spengler, N. Dubilier, M. Liebeke, Spatial metabolomics of in situ host–microbe interactions at the micrometre scale, Nat. Microbiol. 5 (2020) 498–510, https://doi.org/10.1038/s41564-019-0664-6.
[11] J. Lovrić, J. Dunevall, A. Larsson, L. Ren, S. Andersson, A. Meibom, P. Malmberg, M.E. Kurczy, A.G. Ewing, Nano secondary ion mass spectrometry imaging of dopamine distribution across nanometer vesicles, ACS Nano 11 (2017) 3446–3455.
[12] Y. Lan, Z. Zhou, Z. Yang, Single Cell mass spectrometry: towards quantification of small molecules in individual cells, Trends Anal. Chem. 174 (2024) 117657.
[13] I. Protsyuk, A.V. Melnik, L.-F. Nothias, L. Rappez, P. Phapale, A.A. Aksenov, A. Bouslimani, S. Ryazanov, P.C. Dorrestein, T. Alexandrov, 3D molecular cartography using LC-MS facilitated by Optimus and 'ili software, Nat. Protoc. 13 (2018) 134–154.
[14] L. Rappez, M. Stadler, S. Triana, R.M. Gathungu, K. Ovchinnikova, P. Phapale, M. Heikenwalder, T. Alexandrov, SpaceM reveals metabolic states of single cells, Nat. Methods 18 (2021) 799–805.
[15] T.D. Nguyen, Y. Lan, S.S. Kane, J.J. Haffner, R. Liu, L.-I. McCall, Z. Yang, Single-cell mass spectrometry enables insight into heterogeneity in infectious disease, Anal. Chem. 94 (2022) 10567–10572.
[16] J.M. Spraggins, K.V. Djambazova, E.S. Rivera, L.G. Migas, E.K. Neumann, A. Fuetterer, J. Suetering, N. Goedecke, A. Ly, R. Van de Plas, R.M. Caprioli, High-performance molecular imaging with MALDI trapped ion-mobility time-of-flight (timsTOF) mass spectrometry, Anal. Chem. 91 (2019) 14552–14560.
[17] N. Garg, M. Wang, E. Hyde, R.R. da Silva, A.V. Melnik, I. Protsyuk, A. Bouslimani, Y.W. Lim, R. Wong, G. Humphrey, G. Ackermann, T. Spivey, S.S. Brouha, N. Bandeira, G.Y. Lin, F. Rohwer, D.J. Conrad, T. Alexandrov, R. Knight, P. C. Dorrestein, Three-dimensional microbiome and metabolome cartography of a diseased human lung, Cell Host Microbe 22 (2017) 705–716.e4.
[18] D.C. Castro, Y.R. Xie, S.S. Rubakhin, E.V. Romanova, J.V. Sweedler, Image-guided MALDI mass spectrometry for high-throughput single-organelle characterization, Nat. Methods 18 (2021) 1233–1238.
[19] J.K. Lukowski, A. Pamreddy, D. Velickovic, G. Zhang, L. Pasa-Tolic, T. Alexandrov, K. Sharma, C.R. Anderton, Kidney precision medicine Project, storage conditions of human kidney tissue sections affect spatial lipidomics analysis reproducibility, J. Am. Soc. Mass Spectrom. 31 (2020) 2538–2546.
[20] M. Shariatgorji, A. Nilsson, E. Fridjonsdottir, T. Vallianatou, P. Källback, L. Katan, J. Sävmarker, I. Mantas, X. Zhang, E. Bezard, P. Svenningsson, L.R. Odell, P. E. Andrén, Comprehensive mapping of neurotransmitter networks by MALDI–MS imaging, Nat. Methods 16 (2019) 1021–1028, https://doi.org/10.1038/s41592-019-0551-3.
[21] N. Wang, J.P. Sarathy, M. Zimmerman, F. Kaya, H. Wang, V. Dartois, C.L. Carter, On-slide heat sterilization enables mass spectrometry imaging of tissue infected with high-threat pathogens outside of biocontainment: a study directed at, J. Am. Soc. Mass Spectrom. 32 (2021) 2664–2674.
[22] H. Tian, L.J. Sparvero, A.A. Amoscato, A. Bloom, H. Bayır, V.E. Kagan, N. Winograd, Gas cluster ion beam time-of-flight secondary ion mass spectrometry high-resolution imaging of cardiolipin speciation in the brain: identification of molecular losses after traumatic injury, Anal. Chem. 89 (2017) 4611–4619.
[23] S.K. Davies, S. Fearn, L.P. Allsopp, F. Harrison, E. Ware, S.P. Diggle, A. Filloux, D. S. McPhail, J.G. Bundy, Visualizing antimicrobials in bacterial biofilms: three-dimensional biochemical imaging using TOF-SIMS, mSphere 2 (2017), https://doi.org/10.1128/mSphere.00211-17.
[24] C.L. Newell, J.-L. Vorng, J.I. MacRae, I.S. Gilmore, A.P. Gould, Cryogenic OrbiSIMS localizes semi-volatile molecules in biological tissues, Angew. Chem., Int. Ed. Engl. 59 (2020) 18194–18200.
[25] Q. Zhou, A. Fülöp, C. Hopf, Recent developments of novel matrices and on-tissue chemical derivatization reagents for MALDI-MSI, Anal. Bioanal. Chem. 413 (2021) 2599–2617.
[26] M. Kompauer, S. Heiles, B. Spengler, Atmospheric pressure MALDI mass spectrometry imaging of tissues and cells at 1.4-μm lateral resolution, Nat. Methods 14 (2017) 90–96.
[27] X. Liang, S. Cao, P. Xie, X. Hu, Y. Lin, J. Liang, S. Zhang, B. Xian, H. Cao, T. Luan, Z. Cai, Three-dimensional imaging of whole-body zebrafish revealed lipid disorders associated with niemann-pick disease type C1, Anal. Chem. 93 (2021) 8178–8187.
[28] Z. Takáts, J.M. Wiseman, B. Gologan, R.G. Cooks, Mass spectrometry sampling under ambient conditions with desorption electrospray ionization, Science 306 (2004) 471–473.
[29] C. Liu, K. Qi, L. Yao, Y. Xiong, X. Zhang, J. Zang, C. Tian, M. Xu, J. Yang, Z. Lin, Y. Lv, W. Xiong, Y. Pan, Imaging of polar and nonpolar species using compact desorption electrospray ionization/postphotoionization mass spectrometry, Anal. Chem. 91 (2019) 6616–6623.
[30] J. Quartier, W. Rao, S. Slade, F. Métral, M. Lapteva, Y.N. Kalia, DESI-MS imaging to visualize spatial distribution of xenobiotics and endogenous lipids in the skin, Int. J. Pharm. 607 (2021) 120967.
[31] J. Laskin, B.S. Heath, P.J. Roach, L. Cazares, O.J. Semmes, Tissue imaging using nanospray desorption electrospray ionization mass spectrometry, Anal. Chem. 84 (2012) 141–148.
[32] X. Tian, B. Xie, Z. Zou, Y. Jiao, L.-E. Lin, C.-L. Chen, C.-C. Hsu, J. Peng, Z. Yang, Multimodal imaging of amyloid plaques: fusion of the single-probe mass spectrometry image and fluorescence microscopy image, Anal. Chem. 91 (2019) 12882–12889, https://doi.org/10.1021/acs.analchem.9b02792.
[33] O.J. Hale, H.J. Cooper, Native mass spectrometry imaging of proteins and protein complexes by nano-DESI, Anal. Chem. 93 (2021) 4619–4627.
[34] J. Lillja, I. Lanekoff, Silver-doped nano-DESI MSI for increased specificity and sensitivity of alkenes, Methods Mol. Biol. 2437 (2022) 241–249.
[35] H. Cui, Q. Wu, Z. Zhao, Y. Wang, H. Lu, Selective capture-based single-cell mass spectrometry for enhancing sphingolipid profiling of neurons with differentiation of cell body from synapse, Anal. Chem. 94 (2022) 15729–15737.
[36] S. Luo, Q. Wu, Y. Li, H. Lu, Per-pixel absolute quantitation for mass spectrometry imaging of endogenous lipidomes by model prediction of mass transfer kinetics in single-probe-based ambient liquid extraction, Talanta 234 (2021) 122654.
[37] J.M. Wiseman, S.M. Puolitaival, Z. Takáts, R.G. Cooks, R.M. Caprioli, Mass spectrometric profiling of intact biological tissue by using desorption electrospray ionization, Angew. Chem., Int. Ed. Engl. 44 (2005) 7094–7097.
[38] S. Ahlawat, Asha, K.K. Sharma, Gut–organ axis: a microbial outreach and networking, Lett. Appl. Microbiol. 72 (2021) 636–668, https://doi.org/10.1111/lam.13333.
[39] H. Tian, S.S.N. Rabbani, J.C. Vickerman, N. Winograd, Multiomics imaging using high-energy water gas cluster ion beam secondary ion mass spectrometry [(H2O) n-GCIB-SIMS] of frozen-hydrated cells and tissue, Anal. Chem. 93 (2021) 7808–7814, https://doi.org/10.1021/acs.analchem.0c05210.
[40] J. Ding, J. Ji, Z. Rabow, T. Shen, J. Folz, C.R. Brydges, S. Fan, X. Lu, S. Mehta, M. R. Showalter, Y. Zhang, R. Araiza, L.R. Bower, K.C.K. Lloyd, O. Fiehn, A metabolome atlas of the aging mouse brain, Nat. Commun. 12 (2021) 6021.
[41] J.A. Gilbert, M.J. Blaser, J. Gregory Caporaso, J.K. Jansson, S.V. Lynch, R. Knight, Current understanding of the human microbiome, Nat. Med. 24 (2018) 392–400, https://doi.org/10.1038/nm.4517.
[42] R.A. Quinn, A.V. Melnik, A. Vrbanac, T. Fu, K.A. Patras, M.P. Christy, Z. Bodai, P. Belda-Ferre, A. Tripathi, L.K. Chung, M. Downes, R.D. Welch, M. Quinn, G. Humphrey, M. Panitchpakdi, K.C. Weldon, A. Aksenov, R. da Silva, J. Avila-Pacheco, C. Clish, S. Bae, H. Mallick, E.A. Franzosa, J. Lloyd-Price, R. Bussell, T. Thron, A.T. Nelson, M. Wang, E. Leszczynski, F. Vargas, J.M. Gauglitz, M. J. Meehan, E. Gentry, T.D. Arthur, A.C. Komor, O. Poulsen, B.S. Boland, J. T. Chang, W.J. Sandborn, M. Lim, N. Garg, J.C. Lumeng, R.J. Xavier, B. I. Kazmierczak, R. Jain, M. Egan, K.E. Rhee, D. Ferguson, M. Raffatellu, H. Vlamakis, G.G. Haddad, D. Siegel, C. Huttenhower, S.K. Mazmanian, R. M. Evans, V. Nizet, R. Knight, P.C. Dorrestein, Global chemical effects of the microbiome include new bile-acid conjugations, Nature 579 (2020) 123–129.
[43] H. Hulme, L.M. Meikle, N. Strittmatter, J.J.J. van der Hooft, J. Swales, R.A. Bragg, V.H. Villar, M.J. Ormsby, S. Barnes, S.L. Brown, A. Dexter, M.T. Kamat, J. C. Komen, D. Walker, S. Milling, E.K. Osterweil, A.S. MacDonald, C.J. Schofield, S. Tardito, J. Bunch, G. Douce, J.M. Edgar, R. Edrada-Ebel, R.J.A. Goodwin, R. Burchmore, D.M. Wall, Microbiome-derived carnitine mimics as previously unknown mediators of gut-brain axis communication, Sci. Adv. 6 (2020) eaax6328.
[44] D.J. Gonzalez, N.M. Haste, A. Hollands, T.C. Fleming, M. Hamby, K. Pogliano, V. Nizet, P.C. Dorrestein, Microbial competition between Bacillus subtilis and Staphylococcus aureus monitored by imaging mass spectrometry, Microbiology 157 (2011) 2485.
[45] C. Tropini, K.A. Earle, K.C. Huang, J.L. Sonnenburg, The gut microbiome: connecting spatial organization to function, Cell Host Microbe 21 (2017) 433–442.
[46] S. Vaidyanathan, J.S. Fletcher, R. Goodacre, N.P. Lockyer, J. Micklefield, J. C. Vickerman, Subsurface biomolecular imaging of Streptomyces coelicolor using secondary ion mass spectrometry, Anal. Chem. 80 (2008) 1942–1951.
[47] S. Ghosal, S.J. Fallon, T.J. Leighton, K.E. Wheeler, M.J. Kristo, I.D. Hutcheon, P. K. Weber, Imaging and 3D elemental characterization of intact bacterial spores by high-resolution secondary ion mass spectrometry, Anal. Chem. 80 (2008) 5986–5992.
[48] S.K. Cohen, M.-S. Aschtgen, J.B. Lynch, S. Koehler, F. Chen, S. Escrig, J. Daraspe, E.G. Ruby, A. Meibom, M. McFall-Ngai, Tracking the cargo of extracellular symbionts into host tissues with correlated electron microscopy and nanoscale secondary ion mass spectrometry imaging, Cell Microbiol. 22 (2020) e13177.
[49] C. Hoang, W. Uritboonthai, L. Hoang, E.M. Billings, A. Aisporna, F.A. Nia, R.J. E. Derks, J.R. Williamson, M. Giera, G. Siuzdak, Tandem mass spectrometry across platforms, Anal. Chem. (2024), https://doi.org/10.1021/acs.analchem.3c05576.
[50] I. Mohanty, H. Mannochio-Russo, J.V. Schweer, Y. El Abiead, W. Bittremieux, S. Xing, R. Schmid, S. Zuffa, F. Vasquez, V.B. Muti, J. Zemlin, O.E. Tovar-Herrera, S. Moraïs, D. Desai, S. Amin, I. Koo, C.W. Turck, I. Mizrahi, P.M. Kris-Etherton, K. S. Petersen, J.A. Fleming, T. Huan, A.D. Patterson, D. Siegel, L.R. Hagey, M. Wang, A.T. Aron, P.C. Dorrestein, The underappreciated diversity of bile acid modifications, Cell (2024), https://doi.org/10.1016/j.cell.2024.02.019.
[51] S. Han, W. Van Treuren, C.R. Fischer, B.D. Merrill, B.C. DeFelice, J.M. Sanchez, S. K. Higginbottom, L. Guthrie, L.A. Fall, D. Dodd, M.A. Fischbach, J.L. Sonnenburg, A metabolomics pipeline for the mechanistic interrogation of the gut microbiome, Nature 595 (2021) 415–420.
[52] R.A. Quinn, K.A. Hagiwara, K. Liu, M. Goudarzi, W. Pathmasiri, L.W. Sumner, T. O. Metz, Bridging the gap between analytical and microbial sciences in microbiome research, mSystems 6 (2021) e0058521.
[53] M.F. Keating, J. Zhang, C.L. Feider, S. Retailleau, R. Reid, A. Antaris, B. Hart, G. Tan, T.E. Milner, K. Miller, L.S. Eberlin, Integrating the MasSpec Pen to the da Vinci Surgical System for In Vivo Tissue Analysis during a Robotic Assisted Porcine Surgery, Anal. Chem. 92 (2020) 11535–11542, https://doi.org/10.1021/acs.analchem.0c02037.
[54] E.C. Randall, B.G.C. Lopez, S. Peng, M.S. Regan, W.M. Abdelmoula, S.S. Basu, S. Santagata, H. Yoon, M.C. Haigis, J.N. Agar, N.L. Tran, W.F. Elmquist, F.

M. White, J.N. Sarkaria, N.Y.R. Agar, Localized metabolomic gradients in patient-derived xenograft models of glioblastoma, Cancer Res. 80 (2020) 1258–1267.
[55] K.E. Zink, M. Dean, J.E. Burdette, L.M. Sanchez, Imaging mass spectrometry reveals crosstalk between the fallopian tube and the ovary that drives primary metastasis of ovarian cancer, ACS Cent. Sci. 4 (2018) 1360–1370.
[56] C. Sun, T. Li, X. Song, L. Huang, Q. Zang, J. Xu, N. Bi, G. Jiao, Y. Hao, Y. Chen, R. Zhang, Z. Luo, X. Li, L. Wang, Z. Wang, Y. Song, J. He, Z. Abliz, Spatially resolved metabolomics to discover tumor-associated metabolic alterations, Proc. Natl. Acad. Sci. U.S.A. 116 (2019) 52–57.
[57] H. Tian, L.J. Sparvero, T.S. Anthonymuthu, W.-Y. Sun, A.A. Amoscato, R.-R. He, H. Bayır, V.E. Kagan, N. Winograd, Successive high-resolution (HO)-GCIB and C-SIMS imaging integrates multi-omics in different cell types in breast cancer tissue, Anal. Chem. 93 (2021) 8143–8151.
[58] Y. Zhang, J. Wang, J. Liu, J. Han, S. Xiong, W. Yong, Z. Zhao, Combination of ESI and MALDI mass spectrometry for qualitative, semi-quantitative and in situ analysis of gangliosides in brain, Sci. Rep. 6 (2016), https://doi.org/10.1038/srep25289.
[59] I.A. Mulder, N. Ogrinc Potočnik, L.A.M. Broos, A. Prop, M.J.H. Wermer, R.M. A. Heeren, A.M.J.M. van den Maagdenberg, Distinguishing core from penumbra by lipid profiles using Mass Spectrometry Imaging in a transgenic mouse model of ischemic stroke, Sci. Rep. 9 (2019), https://doi.org/10.1038/s41598-018-37612-5.
[60] E. Tanaka, Y. Ogawa, R. Fujii, T. Shimonaka, Y. Sato, T. Hamazaki, T. Nagamura-Inoue, H. Shintaku, M. Tsuji, Metabolomic analysis and mass spectrometry imaging after neonatal stroke and cell therapies in mouse brains, Sci. Rep. 10 (2020) 21881.
[61] T. Zhu, L. Wang, F. Tian, X. Zhao, X.-P. Pu, G.-B. Sun, X.-B. Sun, Anti-ischemia/reperfusion injury effects of notoginsenoside R1 on small molecule metabolism in rat brain after ischemic stroke as visualized by MALDI–MS imaging, Biomed. Pharmacother. 129 (2020) 110470, https://doi.org/10.1016/j.biopha.2020.110470.
[62] L.J. Sparvero, H. Tian, A.A. Amoscato, W.-Y. Sun, T.S. Anthonymuthu, Y. Y. Tyurina, O. Kapralov, S. Javadov, R.-R. He, S.C. Watkins, N. Winograd, V. E. Kagan, H. Bayır, Direct mapping of phospholipid ferroptotic death signals in cells and tissues by gas cluster ion beam secondary ion mass spectrometry (GCIB-SIMS), Angew. Chem., Int. Ed. Engl. 60 (2021) 11784–11788.
[63] K. Mallah, J. Quanico, D. Trede, F. Kobeissy, K. Zibara, M. Salzet, I. Fournier, Lipid changes associated with traumatic brain injury revealed by 3D MALDI-MSI, Anal. Chem. 90 (2018) 10568–10576.
[64] D.C. Barbacci, A. Roux, L. Muller, S.N. Jackson, J. Post, K. Baldwin, B. Hoffer, C. D. Balaban, J.A. Schultz, S. Gouty, B.M. Cox, A.S. Woods, Mass spectrometric imaging of ceramide biomarkers tracks therapeutic response in traumatic brain injury, ACS Chem. Neurosci. 8 (2017) 2266–2274.
[65] A.J. Scott, J.M. Post, R. Lerner, S.R. Ellis, J. Lieberman, K.A. Shirey, R.M. A. Heeren, L. Bindila, R.K. Ernst, Host-based lipid inflammation drives pathogenesis in Francisella infection, Proc. Natl. Acad. Sci. USA 114 (2017) 12596–12601, https://doi.org/10.1073/pnas.1712887114.
[66] W.J. Perry, J.M. Spraggins, J.R. Sheldon, C.M. Grunenwald, D.E. Heinrichs, J. E. Cassat, E.P. Skaar, R.M. Caprioli, Staphylococcus aureusexhibits heterogeneous siderophore production within the vertebrate host, Proc. Natl. Acad. Sci. USA 116 (2019) 21980–21982, https://doi.org/10.1073/pnas.1913991116.
[67] W.J. Perry, C.M. Grunenwald, R. Van de Plas, J.C. Witten, D.R. Martin, S.S. Apte, J.E. Cassat, G.B. Pettersson, R.M. Caprioli, E.P. Skaar, J.M. Spraggins, Visualizing Staphylococcus aureus pathogenic membrane modification within the host infection environment by multimodal imaging mass spectrometry, Cell Chem. Biol. 29 (2022) 1209–1217, e4.
[68] E.J. Lanni, R.N. Masyuko, C.M. Driscoll, J.T. Aerts, J.D. Shrout, P.W. Bohn, J. V. Sweedler, MALDI-guided SIMS: multiscale imaging of metabolites in bacterial biofilms, Anal. Chem. 86 (2014) 9139–9145.
[69] A.G. Wexler, E.R. Guiberson, W.N. Beavers, J.A. Shupe, M. Kay Washington, D. Borden Lacy, R.M. Caprioli, J.M. Spraggins, E.P. Skaar, Clostridioides difficile infection induces a rapid influx of bile acids into the gut during colonization of the host, Cell Rep. 36 (2021) 109683, https://doi.org/10.1016/j.celrep.2021.109683.
[70] N. Strittmatter, P. Kanvatirth, P. Inglese, A.M. Race, A. Nilsson, A. Dannhorn, H. Kudo, R.D. Goldin, S. Ling, E. Wong, F. Seeliger, M.P. Serra, S. Hoffmann, G. Maglennon, G. Hamm, J. Atkinson, S. Jones, J. Bunch, P.E. Andrén, Z. Takats, R.J.A. Goodwin, P. Mastroeni, Holistic characterization of a typhimurium infection model using integrated molecular imaging, J. Am. Soc. Mass Spectrom. 32 (2021) 2791–2802.
[71] A.V. Melnik, Y. Vázquez-Baeza, A.A. Aksenov, E. Hyde, A.C. McAvoy, M. Wang, R.R. da Silva, I. Protsyuk, J.V. Wu, A. Bouslimani, Y.W. Lim, T. Luzzatto-Knaan, W. Comstock, R.A. Quinn, R. Wong, G. Humphrey, G. Ackermann, T. Spivey, S. S. Brouha, N. Bandeira, G.Y. Lin, F. Rohwer, D.J. Conrad, T. Alexandrov, R. Knight, P.C. Dorrestein, N. Garg, Molecular and microbial microenvironments in chronically diseased lungs associated with cystic fibrosis, mSystems 4 (2019), https://doi.org/10.1128/mSystems.00375-19.
[72] D.A. Dean, G. Gautham, J.L. Siqueira-Neto, J.H. McKerrow, P.C. Dorrestein, L.-I. McCall, Spatial metabolomics identifies localized chemical changes in heart tissue during chronic cardiac Chagas Disease, PLoS Neglected Trop. Dis. 15 (2021) e0009819.
[73] E. Hossain, S. Khanam, D.A. Dean, C. Wu, S. Lostracco-Johnson, D. Thomas, S. S. Kane, A.R. Parab, K. Flores, M. Katemauswa, C. Gosmanov, S.E. Hayes, Y. Zhang, D. Li, C. Woelfel-Monsivais, K. Sankaranarayanan, L.-I. McCall, Mapping of host-parasite-microbiome interactions reveals metabolic determinants of tropism and tolerance in Chagas disease, Sci. Adv. 6 (2020) eaaz2015.
[74] K. Hoffman, Z. Liu, E. Hossain, M.E. Bottazzi, P.J. Hotez, K.M. Jones, L.-I. McCall, Alterations to the cardiac metabolome induced by chronic infection relate to the degree of cardiac pathology, ACS Infect. Dis. 7 (2021) 1638–1649.
[75] N.H. Patterson, M. Tuck, A. Lewis, A. Kaushansky, J.L. Norris, R. Van de Plas, R. M. Caprioli, Next generation histology-directed imaging mass spectrometry driven by autofluorescence microscopy, Anal. Chem. 90 (2018) 12404–12413.
[76] N. Desbenoit, I. Schmitz-Afonso, C. Baudouin, O. Laprévote, D. Touboul, F. Brignole-Baudouin, A. Brunelle, Localisation and quantification of benzalkonium chloride in eye tissue by TOF-SIMS imaging and liquid chromatography mass spectrometry, Anal. Bioanal. Chem. 405 (2013) 4039–4049.
[77] N. Mori, T. Mochizuki, F. Yamazaki, S. Takei, H. Mano, T. Matsugi, M. Setou, MALDI imaging mass spectrometry revealed atropine distribution in the ocular tissues and its transit from anterior to posterior regions in the whole-eye of rabbit after topical administration, PLoS One 14 (2019) e0211376.
[78] A. Balla, S. Auriola, A.C. Grey, N.J. Demarais, A. Valtari, E.M. Heikkinen, E. Toropainen, A. Urtti, K.-S. Vellonen, M. Ruponen, Partitioning and spatial distribution of drugs in ocular surface tissues, Pharmaceutics 13 (2021), https://doi.org/10.3390/pharmaceutics13050658.
[79] B. Prideaux, V. Dartois, D. Staab, D.M. Weiner, A. Goh, L.E. Via, C.E. Barry, M. Stoeckli, High-sensitivity MALDI-MRM-MS imaging of moxifloxacin distribution in tuberculosis-infected rabbit lungs and granulomatous lesions, Anal. Chem. 83 (2011) 2112–2118.
[80] A.S. Mokosch, S. Gerbig, C.G. Grevelding, S. Haeberlein, B. Spengler, High-resolution AP-SMALDI MSI as a tool for drug imaging in Schistosoma mansoni, Anal. Bioanal. Chem. 413 (2021) 2755–2766.
[81] H.K. Seneviratne, A.N. Hamlin, C.J.S. Heck, N.N. Bumpus, Spatial distribution profiles of emtricitabine, tenofovir, efavirenz, and rilpivirine in murine tissues following in vivo dosing correlate with their safety profiles in humans, ACS Pharmacol. Transl. Sci. 3 (2020) 655–665, https://doi.org/10.1021/acsptsci.0c00015.
[82] V. Pareek, H. Tian, N. Winograd, S.J. Benkovic, Metabolomics and mass spectrometry imaging reveal channeled de novo purine synthesis in cells, Science 368 (2020) 283–290, https://doi.org/10.1126/science.aaz6465.
[83] Z. Yuan, Q. Zhou, L. Cai, L. Pan, W. Sun, S. Qumu, S. Yu, J. Feng, H. Zhao, Y. Zheng, M. Shi, S. Li, Y. Chen, X. Zhang, M.Q. Zhang, SEAM is a spatial single nuclear metabolomics method for dissecting tissue microenvironment, Nat. Methods 18 (2021) 1223–1232.
[84] M. Niehaus, J. Soltwisch, M.E. Belov, K. Dreisewerd, Transmission-mode MALDI-2 mass spectrometry imaging of cells and tissues at subcellular resolution, Nat. Methods 16 (2019) 925–931.
[85] K.V. Djambazova, D.R. Klein, L.G. Migas, E.K. Neumann, E.S. Rivera, R. Van de Plas, R.M. Caprioli, J.M. Spraggins, Resolving the complexity of spatial lipidomics using MALDI TIMS imaging mass spectrometry, Anal. Chem. 92 (2020) 13290–13297.
[86] L.-X. Jiang, E. Hernly, H. Hu, R.T. Hilger, H. Neuweger, M. Yang, J. Laskin, Nanospray desorption electrospray ionization (Nano-DESI) mass spectrometry imaging with high ion mobility resolution, J. Am. Soc. Mass Spectrom. 34 (2023) 1798–1804.
[87] T. Porta, E. Varesio, G. Hopfgartner, Gas-phase separation of drugs and metabolites using modifier-assisted differential ion mobility spectrometry hyphenated to liquid extraction surface analysis and mass spectrometry, Anal. Chem. 85 (2013) 11771–11779.
[88] Z. Liu, R. Ulrich vonBargen, A.L. Kendricks, K. Wheeler, A.C. Leão, K. Sankaranarayanan, D.A. Dean, S.S. Kane, E. Hossain, J. Pollet, M.E. Bottazzi, P. J. Hotez, K.M. Jones, L.-I. McCall, Localized cardiac small molecule trajectories and persistent chemical sequelae in experimental Chagas disease, Nat. Commun. 14 (2023) 6769.
[89] K. Dührkop, L.-F. Nothias, M. Fleischauer, R. Reher, M. Ludwig, M.A. Hoffmann, D. Petras, W.H. Gerwick, J. Rousu, P.C. Dorrestein, S. Böcker, Systematic classification of unknown metabolites using high-resolution fragmentation mass spectra, Nat. Biotechnol. 39 (2021) 462–471.
[90] A. Palmer, P. Phapale, I. Chernyavsky, R. Lavigne, D. Fay, A. Tarasov, V. Kovalev, J. Fuchser, S. Nikolenko, C. Pineau, M. Becker, T. Alexandrov, FDR-controlled metabolite annotation for high-resolution imaging mass spectrometry, Nat. Methods 14 (2017) 57–60.
[91] S.R. Ellis, M.R.L. Paine, G.B. Eijkel, J.K. Pauling, P. Husen, M.W. Jervelund, M. Hermansson, C.S. Ejsing, R.M.A. Heeren, Automated, parallel mass spectrometry imaging and structural identification of lipids, Nat. Methods 15 (2018) 515–518.
[92] D. Unsihuay, R. Yin, D.M. Sanchez, M. Yang, Y. Li, X. Sun, S.K. Dey, J. Laskin, High-resolution imaging and identification of biomolecules using Nano-DESI coupled to ion mobility spectrometry, Anal. Chim. Acta 1186 (2021) 339085.
[93] W. Michno, P.M. Wehrli, S. Koutarapu, C. Marsching, K. Minta, J. Ge, S.W. Meyer, H. Zetterberg, K. Blennow, C. Henkel, J. Oetjen, C. Hopf, J. Hanrieder, Structural amyloid plaque polymorphism is associated with distinct lipid accumulations revealed by trapped ion mobility mass spectrometry imaging, J. Neurochem. 160 (2022) 482–498.
[94] B.A. Dilmetz, Y. Lee, M.R. Condina, M. Briggs, C. Young, C.T. Desire, M. Klingler-Hoffmann, P. Hoffmann, Novel technical developments in mass spectrometry imaging in 2020: a mini review, Anal. Sci. Adv. 2 (2021) 225–237, https://doi.org/10.1002/ansa.202000176.
[95] E.M. Llufrio, L. Wang, F.J. Naser, G.J. Patti, Sorting cells alters their redox state and cellular metabolome, Redox Biol. 16 (2018) 381–387.

[96] Y. Matsuoka, M. Takahashi, Y. Sugiura, Y. Izumi, K. Nishiyama, M. Nishida, M. Suematsu, T. Bamba, K.-I. Yamada, Structural library and visualization of endogenously oxidized phosphatidylcholines using mass spectrometry-based techniques, Nat. Commun. 12 (2021) 6339.

[97] H. Yu, S. Xing, L. Nierves, P.F. Lange, T. Huan, Fold-change compression: an unexplored but correctable quantitative bias caused by nonlinear electrospray ionization responses in untargeted metabolomics, Anal. Chem. 92 (2020) 7011–7019.

[98] T. Ghosh, D. Philtron, W. Zhang, K. Kechris, D. Ghosh, Reproducibility of mass spectrometry based metabolomics data, BMC Bioinf. 22 (2021) 423.

[99] T. Boskamp, R. Casadonte, L. Hauberg-Lotte, S. Deininger, J. Kriegsmann, P. Maass, Cross-normalization of MALDI mass spectrometry imaging data improves site-to-site reproducibility, Anal. Chem. 93 (2021) 10584–10592.

[100] A.M. Race, A. Rae, J.-L. Vorng, R. Havelund, A. Dexter, N. Kumar, R.T. Steven, M. K. Passarelli, B.J. Tyler, J. Bunch, I.S. Gilmore, Correlative hyperspectral imaging using a dimensionality-reduction-based image fusion method, Anal. Chem. 92 (2020) 10979–10988.

[101] E. Fahy, S. Subramaniam, RefMet: a reference nomenclature for metabolomics, Nat. Methods 17 (2020) 1173–1174.

[102] G. Liebisch, E. Fahy, J. Aoki, E.A. Dennis, T. Durand, C.S. Ejsing, M. Fedorova, I. Feussner, W.J. Griffiths, H. Köfeler, A.H. Merrill Jr., R.C. Murphy, V. B. O'Donnell, O. Oskolkova, S. Subramaniam, M.J.O. Wakelam, F. Spener, Update on LIPID MAPS classification, nomenclature, and shorthand notation for MS-derived lipid structures, J. Lipid Res. 61 (2020) 1539–1555.

[103] J.T. Morton, A.A. Aksenov, L.F. Nothias, J.R. Foulds, R.A. Quinn, M.H. Badri, T. L. Swenson, M.W. Van Goethem, T.R. Northen, Y. Vazquez-Baeza, M. Wang, N. A. Bokulich, A. Watters, S.J. Song, R. Bonneau, P.C. Dorrestein, R. Knight, Learning representations of microbe-metabolite interactions, Nat. Methods 16 (2019) 1306–1314.

[104] D.G. Barnes, M. Vidiassov, B. Ruthensteiner, C.J. Fluke, M.R. Quayle, C. R. McHenry, Embedding and publishing interactive, 3-dimensional, scientific figures in Portable Document Format (PDF) files, PLoS One 8 (2013) e69446.

[105] M. Woolman, J. Qiu, C.M. Kuzan-Fischer, I. Ferry, D. Dara, L. Katz, F. Daud, M. Wu, M. Ventura, N. Bernards, H. Chan, I. Fricke, M. Zaidi, B.G. Wouters, J. T. Rutka, S. Das, J. Irish, R. Weersink, H.J. Ginsberg, D.A. Jaffray, A. Zarrine-Afsar, Tissue pathology from spatially encoded mass spectrometry classifiers visualized in real time through augmented reality, Chem. Sci. 11 (2020) 8723–8735.

[106] P. Wolle, M.P. Müller, D. Rauh, Augmented reality in scientific publications—taking the visualization of 3D structures to the next level, ACS Chem. Biol. 13 (2018) 496–499, https://doi.org/10.1021/acschembio.8b00153.

[107] J.K. Aw, K.C. Boellaard, T.K. Tan, J. Yap, Y.P. Loh, B. Colasson, É. Blanc, Y. Lam, F.M. Fung, Interacting with three-dimensional molecular structures using an augmented reality mobile app, J. Chem. Educ. 97 (2020) 3877–3881, https://doi.org/10.1021/acs.jchemed.0c00387.

[108] M. Wang, J.J. Carver, V.V. Phelan, L.M. Sanchez, N. Garg, Y. Peng, D.D. Nguyen, J. Watrous, C.A. Kapono, T. Luzzatto-Knaan, C. Porto, A. Bouslimani, A.V. Melnik, M.J. Meehan, W.-T. Liu, M. Crüsemann, P.D. Boudreau, E. Esquenazi, M. Sandoval-Calderón, R.D. Kersten, L.A. Pace, R.A. Quinn, K.R. Duncan, C.-C. Hsu, D.J. Floros, R.G. Gavilan, K. Kleigrewe, T. Northen, R.J. Dutton, D. Parrot, E.E. Carlson, B. Aigle, C.F. Michelsen, L. Jelsbak, C. Sohlenkamp, P. Pevzner, A. Edlund, J. McLean, J. Piel, B.T. Murphy, L. Gerwick, C.-C. Liaw, Y.-L. Yang, H.-U. Humpf, M. Maansson, R.A. Keyzers, A.C. Sims, A.R. Johnson, A.M. Sidebottom, B.E. Sedio, A. Klitgaard, C.B. Larson, C.A.B. P, D. Torres-Mendoza, D.J. Gonzalez, D.B. Silva, L.M. Marques, D.P. Demarque, E. Pociute, E.C. O'Neill, E. Briand, E.J. N. Helfrich, E.A. Granatosky, E. Glukhov, F. Ryffel, H. Houson, H. Mohimani, J. J. Kharbush, Y. Zeng, J.A. Vorholt, K.L. Kurita, P. Charusanti, K.L. McPhail, K. F. Nielsen, L. Vuong, M. Elfeki, M.F. Traxler, N. Engene, N. Koyama, O.B. Vining, R. Baric, R.R. Silva, S.J. Mascuch, S. Tomasi, S. Jenkins, V. Macherla, T. Hoffman, V. Agarwal, P.G. Williams, J. Dai, R. Neupane, J. Gurr, A.M.C. Rodríguez, A. Lamsa, C. Zhang, K. Dorrestein, B.M. Duggan, J. Almaliti, P.-M. Allard, P. Phapale, L.-F. Nothias, T. Alexandrov, M. Litaudon, J.-L. Wolfender, J.E. Kyle, T.O. Metz, T. Peryea, D.-T. Nguyen, D. VanLeer, P. Shinn, A. Jadhav, R. Müller, K. M. Waters, W. Shi, X. Liu, L. Zhang, R. Knight, P.R. Jensen, B.O. Palsson, K. Pogliano, R.G. Linington, M. Gutiérrez, N.P. Lopes, W.H. Gerwick, B.S. Moore, P.C. Dorrestein, N. Bandeira, Sharing and community curation of mass spectrometry data with global natural products social molecular networking, Nat. Biotechnol. 34 (2016) 828–837.

[109] M. Sud, E. Fahy, D. Cotter, K. Azam, I. Vadivelu, C. Burant, A. Edison, O. Fiehn, R. Higashi, K.S. Nair, S. Sumner, S. Subramaniam, Metabolomics Workbench: an international repository for metabolomics data and metadata, metabolite standards, protocols, tutorials and training, and analysis tools, Nucleic Acids Res. 44 (2016) D463–D470.

[110] K. Haug, K. Cochrane, V.C. Nainala, M. Williams, J. Chang, K.V. Jayaseelan, C. O'Donovan, MetaboLights: a resource evolving in response to the needs of its scientific community, Nucleic Acids Res. 48 (2020) D440–D444.

[111] C.M. Lewis Jr., L.-I. McCall, R.R. Sharp, P.G. Spicer, Ethical priority of the most actionable system of biomolecules: the metabolome, Am. J. Phys. Anthropol. 171 (2020) 177–181.

[112] M.C. Föll, L. Moritz, T. Wollmann, M.N. Stillger, N. Vockert, M. Werner, P. Bronsert, K. Rohr, B.A. Grüning, O. Schilling, Accessible and reproducible mass spectrometry imaging data analysis in Galaxy, GigaScience 8 (2019), https://doi.org/10.1093/gigascience/giz143.

[113] L.W. Sumner, A. Amberg, D. Barrett, M.H. Beale, R. Beger, C.A. Daykin, T.W.-M. Fan, O. Fiehn, R. Goodacre, J.L. Griffin, T. Hankemeier, N. Hardy, J. Harnly, R. Higashi, J. Kopka, A.N. Lane, J.C. Lindon, P. Marriott, A.W. Nicholls, M. D. Reily, J.J. Thaden, M.R. Viant, Proposed minimum reporting standards for chemical analysis, Metabolomics 3 (2007) 211–221, https://doi.org/10.1007/s11306-007-0082-2.

[114] L.A. McDonnell, A. Römpp, B. Balluff, R.M.A. Heeren, J.P. Albar, P.E. Andrén, G. L. Corthals, A. Walch, M. Stoeckli, Discussion point: reporting guidelines for mass spectrometry imaging, Anal. Bioanal. Chem. 407 (2015) 2035–2045.

[115] O.J.R. Gustafsson, L.J. Winderbaum, M.R. Condina, B.A. Boughton, B. R. Hamilton, E.A.B. Undheim, M. Becker, P. Hoffmann, Balancing sufficiency and impact in reporting standards for mass spectrometry imaging experiments, GigaScience 7 (2018), https://doi.org/10.1093/gigascience/giy102.

[116] J. Woodford, A. Gillman, P. Jenvey, J. Roberts, S. Woolley, B.E. Barber, M. Fernandez, S. Rose, P. Thomas, N.M. Anstey, J.S. McCarthy, Positron emission tomography and magnetic resonance imaging in experimental human malaria to identify organ-specific changes in morphology and glucose metabolism: a prospective cohort study, PLoS Med. 18 (2021) e1003567.

[117] I.M. Jackson, S.J. Lee, A.R. Sowa, M.E. Rodnick, L. Bruton, M. Clark, S. Preshlock, J. Rothley, V.E. Rogers, L.E. Botti, B.D. Henderson, B.G. Hockley, J. Torres, D. M. Raffel, A.F. Brooks, K.A. Frey, M.R. Kilbourn, R.A. Koeppe, X. Shao, P.J. H. Scott, Use of 55 PET radiotracers under approval of a radioactive drug research committee (RDRC), EJNMMI Radiopharm. Chem. 5 (2020) 24.

[118] I.K. Lee, D.A. Jacome, J.K. Cho, V. Tu, A.J. Young, T. Dominguez, J.D. Northrup, J.M. Etersque, H.S. Lee, A. Ruff, O. Aklilu, K. Bittinger, L.J. Glaser, D. Dorgan, D. Hadjiliadis, R.M. Kohli, R.H. Mach, D.A. Mankoff, R.K. Doot, M.A. Sellmyer, Imaging sensitive and drug-resistant bacterial infection with [11C]-trimethoprim, J. Clin. Invest. 132 (2022), https://doi.org/10.1172/JCI156679.

[119] M. Tzafetas, A. Mitra, M. Paraskevaidi, Z. Bodai, I. Kalliala, S. Bowden, K. Lathouras, F. Rosini, M. Szasz, A. Savage, E. Manoli, J. Balog, J. McKenzie, D. Lyons, P. Bennett, D. MacIntyre, S. Ghaem-Maghami, Z. Takats, M. Kyrgiou, The intelligent knife (iKnife) and its intraoperative diagnostic advantage for the treatment of cervical disease, Proc. Natl. Acad. Sci. U.S.A. 117 (2020) 7338–7346.

[120] J. Balog, L. Sasi-Szabó, J. Kinross, M.R. Lewis, L.J. Muirhead, K. Veselkov, R. Mirnezami, B. Dezső, L. Damjanovich, A. Darzi, J.K. Nicholson, Z. Takáts, Intraoperative tissue identification using rapid evaporative ionization mass spectrometry, Sci. Transl. Med. 5 (2013) 194ra93.

[121] J. Zhang, J. Rector, J.Q. Lin, J.H. Young, M. Sans, N. Katta, N. Giese, W. Yu, C. Nagi, J. Suliburk, J. Liu, A. Bensussan, R.J. DeHoog, K.Y. Garza, B. Ludolph, A. G. Sorace, A. Syed, A. Zahedivash, T.E. Milner, L.S. Eberlin, Nondestructive tissue analysis for ex vivo and in vivo cancer diagnosis using a handheld mass spectrometry system, Sci. Transl. Med. 9 (2017), https://doi.org/10.1126/scitranslmed.aan3968.

[122] M.E. King, J. Zhang, J.Q. Lin, K.Y. Garza, R.J. DeHoog, C.L. Feider, A. Bensussan, M. Sans, A. Krieger, S. Badal, M.F. Keating, S. Woody, S. Dhingra, W. Yu, C. Pirko, K.A. Brahmbhatt, G. Van Buren, W.E. Fisher, J. Suliburk, L.S. Eberlin, Rapid diagnosis and tumor margin assessment during pancreatic cancer surgery with the MasSpec Pen technology, Proc. Natl. Acad. Sci. U.S.A. 118 (2021), https://doi.org/10.1073/pnas.2104411118.

[123] V. Pirro, C.M. Alfaro, A.K. Jarmusch, E.M. Hattab, A.A. Cohen-Gadol, R.G. Cooks, Intraoperative assessment of tumor margins during glioma resection by desorption electrospray ionization-mass spectrometry, Proc. Natl. Acad. Sci. U.S. A. 114 (2017) 6700–6705.

[124] P. Rajbhandari, T.V. Neelakantan, N. Hosny, B.R. Stockwell, Spatial pharmacology using mass spectrometry imaging, Trends Pharmacol. Sci. 45 (2024) 67–80.

[125] M.L. Spruill, M. Maletic-Savatic, H. Martin, F. Li, X. Liu, Spatial analysis of drug absorption, distribution, metabolism, and toxicology using mass spectrometry imaging, Biochem. Pharmacol. 201 (2022) 115080.

[126] E.J.N. Helfrich, C.M. Vogel, R. Ueoka, M. Schäfer, F. Ryffel, D.B. Müller, S. Probst, M. Kreuzer, J. Piel, J.A. Vorholt, Bipartite interactions, antibiotic production and biosynthetic potential of the Arabidopsis leaf microbiome, Nat. Microbiol. 3 (2018) 909–919.

[127] V.V. Phelan, J. Fang, P.C. Dorrestein, Mass spectrometry analysis of Pseudomonas aeruginosa treated with azithromycin, J. Am. Soc. Mass Spectrom. 26 (2015) 873–877.

[128] E.V. Vonhof, M. Piotto, E. Holmes, J.C. Lindon, J.K. Nicholson, J.V. Li, Improved spatial resolution of metabolites in tissue biopsies using high-resolution magic-angle-spinning slice localization NMR spectroscopy, Anal. Chem. 92 (2020) 11516–11519.

[129] J. Du, Y. Su, C. Qian, D. Yuan, K. Miao, D. Lee, A.H.C. Ng, R.S. Wijker, A. Ribas, R. D. Levine, J.R. Heath, L. Wei, Raman-guided subcellular pharmaco-metabolomics for metastatic melanoma cells, Nat. Commun. 11 (2020) 4830.